


# Light Higgs boson in the NMSSM confronted with the CMS di-photon and di-tau excesses\*

Weichao Li (李为超)<sup>1</sup> Haoxue Qiao (乔豪学)<sup>1†</sup> Jingya Zhu (朱经亚)<sup>2‡</sup> 

<sup>1</sup>School of Physics and Technology, Wuhan University, Wuhan 430072, China

<sup>2</sup>Joint Center for Theoretical Physics, and School of Physics and Electronics, Henan University, Kaifeng 475004, China

**Abstract:** In 2018, the CMS collaboration reported a di-photon excess at approximately 95.3 GeV with a local significance of  $2.8\sigma$ . Interestingly, the CMS collaboration also recently reported a di-tau excess at 95–100 GeV with a local significance of  $2.6–3.1\sigma$ . In addition, a  $b\bar{b}$  excess at 98 GeV with a local significance of  $2.3\sigma$  was reported from LEP data approximately twenty years ago. In this study, we addressed the interpretation of these excesses together with a light Higgs boson in the next-to-minimal supersymmetric standard model (NMSSM). We conclude that, in the NMSSM, the 95–100 GeV excesses are difficult to be satisfied simultaneously (not possible globally at the  $1\sigma$  level or simultaneously at the  $2\sigma$  level). We analyzed two partially-satisfied scenarios: global  $2\sigma$  and small di-photon. An approximate equation of global fit to the three excesses was derived, and two representative types of surviving samples were analyzed in detail. Given that the mass regions of these excesses are near the  $Z$  boson, we also checked the light Higgs boson in the  $t\bar{t}$ -associated channels. The detailed results may be useful for further checking the low-mass-region excesses in the future.

**Keywords:** Higgs boson, supersymmetry phenomenology, NMSSM

**DOI:** 10.1088/1674-1137/acfaf1

## I. INTRODUCTION

In 2012, the ATLAS and CMS collaborations reported that a new boson at approximately 125 GeV was discovered at the LHC [1, 2]. It was proved to be the Standard Model (SM)-like Higgs boson, according to its spin,  $CP$  property, production, and decay performances in Run I and Run II data globally [3–5]. The Higgs boson is related to the electroweak symmetry-breaking mechanism and hierarchy problem and represents an interesting phenomenology in many new physics models. The question of whether there are additional Higgs bosons is natural, important, and remains unsolved. Ten years after the 125-GeV Higgs boson was discovered, experimentalists are still making efforts to search for additional Higgs scalars, even if in the low-mass region.

In 2018, the CMS collaboration reported a di-photon excess at approximately 95.3 GeV with a local significance of  $2.8\sigma$  [6] and a signal strength of

$$R_{\gamma\gamma}^{\text{ex}} = \frac{\sigma^{\text{ex}}(gg \rightarrow \phi \rightarrow \gamma\gamma)}{\sigma^{\text{SM}}(gg \rightarrow h \rightarrow \gamma\gamma)} = 0.6 \pm 0.2. \quad (1)$$

Interestingly, the CMS collaboration recently also reported a di-tau excess at 95–100 GeV with a local significance of  $2.6–3.1\sigma$  [7] and a signal strength of

$$R_{\tau\tau}^{\text{ex}} = \frac{\sigma^{\text{ex}}(gg \rightarrow \phi \rightarrow \tau^+\tau^-)}{\sigma^{\text{SM}}(gg \rightarrow h \rightarrow \tau^+\tau^-)} = 1.2 \pm 0.5. \quad (2)$$

Besides, a  $b\bar{b}$  excess at approximately 98 GeV with a local significance of  $2.3\sigma$  was reported from the LEP data approximately twenty years ago [8], whose signal strength is

$$R_{bb}^{\text{ex}} = \frac{\sigma^{\text{ex}}(e^+e^- \rightarrow Z\phi \rightarrow Zb\bar{b})}{\sigma^{\text{SM}}(e^+e^- \rightarrow Zh \rightarrow Zb\bar{b})} = 0.117 \pm 0.057. \quad (3)$$

Given that the three excesses are close to each other in mass regions and comparable in signal strengths with a SM Higgs boson of the same mass, a series of studies

Received 14 July 2023; Accepted 18 September 2023; Published online 19 September 2023

\* Supported by the National Natural Science Foundation of China (12275066, 11605123, 11547103, 12074295)

<sup>†</sup> E-mail: qhx@whu.edu.cn

<sup>‡</sup> E-mail: zhujy@henu.edu.cn



Content from this work may be used under the terms of the Creative Commons Attribution 3.0 licence. Any further distribution of this work must maintain attribution to the author(s) and the title of the work, journal citation and DOI. Article funded by SCOAP<sup>3</sup> and published under licence by Chinese Physical Society and the Institute of High Energy Physics of the Chinese Academy of Sciences and the Institute of Modern Physics of the Chinese Academy of Sciences and IOP Publishing Ltd

were conducted to interpret them as one additional Higgs-like scalar in new physics models, with [9–12] and without [13–32] di-tau excess.

Supersymmetry (SUSY) [33–35] is a popular theory beyond the SM. The next-to-minimal supersymmetric standard model (NMSSM) [36] includes two Higgs doublets and one singlet, which implies more freedom than the minimal supersymmetric standard model (MSSM) in the Higgs sector [37]. It can naturally accommodate a SM-like Higgs boson at 125 GeV with signal strengths properly fitting the experimental data [38–47]. It can also predict a type of Higgs exotic decay to a pair of additional Higgs scalars lighter than the half mass [48–51]. At the moment, we have three possible excesses in different channels in the 95–100 GeV region. Thus, it is interesting to analyze whether it is possible to interpret all three excesses together in the NMSSM. In this study, we imposed the three excesses from one 95–100 GeV Higgs scalar in NMSSM, investigating its status by confronting the excesses. In our calculations, we considered other related constraints including Higgs data, SUSY searches, dark matter relic density, and direct detection.

The rest of this paper is organized as follows. In Sec. II, we introduce the Higgs sector in NMSSM and present the relevant analytic equations. In Sec. III, we report and discuss numerical-calculation results. Finally, we draw the main conclusions in Sec. IV.

## II. THE HIGGS SECTOR IN NMSSM

SUSY models are mainly determined by their superpotential and soft-breaking terms. In the NMSSM, they can be written as

$$W = W_{\text{MSSM}}^{\mu \rightarrow \lambda \hat{S}} + \kappa \hat{S}^3 / 3, \quad (4)$$

$$V_{\text{soft}} = \tilde{m}_{H_u}^2 |H_u|^2 + \tilde{m}_{H_d}^2 |H_d|^2 + \tilde{m}_S^2 |S|^2 + (\lambda A_\lambda S H_u \cdot H_d + \kappa A_\kappa S^3 / 3 + \text{h.c.}), \quad (5)$$

where  $W_{\text{MSSM}}^{\mu \rightarrow \lambda \hat{S}}$  is the MSSM superpotential with the  $\mu$ -term generated effectively by the Vacuum Expectation Value (VEV) of singlet field, and  $\tilde{m}_{H_u}$ ,  $\tilde{m}_{H_d}$ ,  $\tilde{m}_S$ ,  $A_\lambda$ , and  $A_\kappa$  are soft-breaking parameters.  $\hat{H}_u$ ,  $\hat{H}_d$  are the  $SU(2)$  doublet and  $\hat{S}$  is the singlet Higgs superfields; after obtaining VEVs, the scalar fields can be expressed as

$$H_u = \begin{pmatrix} H_u^+ \\ v_u + \frac{\phi_u + i\varphi_u}{\sqrt{2}} \end{pmatrix},$$

$$H_d = \begin{pmatrix} v_d + \frac{\phi_d + i\varphi_d}{\sqrt{2}} \\ H_d^- \end{pmatrix}, \quad S = v_s + \frac{\phi_s + i\varphi_s}{\sqrt{2}}, \quad (6)$$

and  $\tan\beta \equiv v_u/v_d$ .

The three gauge-eigenstate scalars  $\{\phi_u, \phi_d, \phi_s\}$  mix to form three  $CP$ -even mass-eigenstate Higgs scalars  $\{h_1, h_2, h_3\}$ , with mass order  $m_{h_1} < m_{h_2} < m_{h_3}$  and mixing matrix  $\{S_{ij}\}_{3 \times 3}$ :

$$\begin{pmatrix} h_1 \\ h_2 \\ h_3 \end{pmatrix} = \begin{pmatrix} S_{11} & S_{12} & S_{13} \\ S_{21} & S_{22} & S_{23} \\ S_{31} & S_{32} & S_{33} \end{pmatrix} \begin{pmatrix} \phi_u \\ \phi_d \\ \phi_s \end{pmatrix}. \quad (7)$$

The reduced couplings of  $h_1$  to up- and down-type fermions, and massive gauge bosons, are given by

$$c_t = S_{11} / \sin\beta,$$

$$c_b = S_{12} / \cos\beta,$$

$$c_V = S_{11} \sin\beta + S_{12} \cos\beta. \quad (8)$$

The loop-induced coupling to gluons  $c_g$  is mainly determined by  $c_t$  and light colored SUSY particles, and that of photon  $c_\gamma$  is mainly determined by  $c_t$ ,  $c_V$ , and light charged SUSY particles.

## III. NUMERICAL RESULTS AND DISCUSSIONS

In the conducted calculations, we first scanned the parameter space of NMSSM with the public code NMSSMTools\_5.6.1 [52–54] under a series of experimental and theoretical constraints<sup>1)</sup>. The parameter space we considered is defined as follows:

$$0.1 < \lambda < 0.7, \quad |\kappa| < 0.7, \quad 1 < \tan\beta < 60,$$

$$M_0, |M_3|, |A_0|, |A_\lambda|, |A_\kappa| < 10 \text{ TeV},$$

$$\mu_{\text{eff}}, |M_1|, |M_2| < 1 \text{ TeV}. \quad (9)$$

Note that the NMSSM considered in this study is GUT-scale constrained, where both Higgs and gaugino masses are considered non-universal. Thus,  $M_0$  and  $A_0$  are the unified sfermion masses and trilinear couplings in the sfermion sector, and  $M_{1,2,3}$  are the gaugino masses at the

<sup>1)</sup> We do not take the constraints to Higgs couplings into account, for these constraints are only global fit results under some assumptions, e.g., no exotic and invisible Higgs decays when varying the couplings. Instead, we use direct experimental constraints to Higgs signals with the code HiggsSignals.

GUT scale. The three non-universal Higgs masses at the GUT scale were calculated from the minimization equations, with  $\lambda$ ,  $\kappa$ , and  $\mu_{\text{eff}} \equiv \lambda v_S$  at the SUSY scale as the input parameters. The parameter  $\mu_{\text{eff}}$  was chosen to be positive to interpret the muon  $g-2$  anomaly. One sign in three of  $M_{1,2,3}$  can be absorbed in a field redefinition [35]. The sign of  $M_3$  can have other effects (see Ref. [55]).

The constraints we imposed include (i) A SM-like Higgs boson<sup>1)</sup> with mass at approximately 125 GeV (i.e., 123 – 127 GeV) and signal strengths in agreement with the latest data in HiggsSignals – 2.2.3beta [56, 57]; (ii) exclusion limits in the search for additional Higgs bosons at the LEP, Tevatron, and LHC, collected from HiggsBounds – 5.10.1 [58–60]; (iii) upper limit of dark matter relic density with uncertainty ( $\Omega h^2 \leq 0.131$ ) [61–63] and direct detections [64], where the quantities were calculated using micrOMEGAs in NMSSMTools; (iv) exclusion limits in SUSY searches imposed in SModelS – v2.1.1 [65–68], such as electroweakinos in multilepton channels [69, 70] and gluino and first-two-generation squarks [71]; and (v) theoretical constraints of vacuum stability and no Landau pole below GUT scale [54].

To interpret the CMS di-photon and di-tau, and LEP  $b\bar{b}$  excesses together, we also require a light Higgs boson of 95 – 100 GeV. For the surviving samples, we defined a chi-square quantity  $\chi_{\gamma\gamma+\tau\tau+bb}^2$  to describe its ability to interpret the three excesses globally:

$$\chi_{\gamma\gamma+\tau\tau+bb}^2 = \chi_{\gamma\gamma}^2 + \chi_{\tau\tau}^2 + \chi_{bb}^2, \quad (10)$$

where

$$\chi_i^2 = \left( \frac{R_i - \bar{R}_i^{\text{ex}}}{\delta R_i^{\text{ex}}} \right)^2,$$

where  $i = \gamma\gamma, \tau\tau, bb$ ,  $R_i$  denotes the corresponding theoretical signal strength of our samples, and  $\bar{R}_i^{\text{ex}}$  and  $\delta R_i^{\text{ex}}$  denote the corresponding experimental mean and error values, respectively. For  $\chi_{\gamma\gamma+\tau\tau+bb}^2 \leq 8.03$ , the surviving samples can interpret the three excesses globally at  $2\sigma$  level. They will be called 'global  $2\sigma$  samples' or alternatively ' $2\sigma$  samples' hereafter. Note that for surviving samples, the minimum value of  $\chi_{\gamma\gamma+\tau\tau+bb}^2$  is 5.37; therefore, there are no samples satisfying the three excesses at  $1\sigma$  level globally ( $\chi_{\gamma\gamma+\tau\tau+bb}^2 < 3.53$ ). Table 1 lists the parameter regions for the  $2\sigma$  and all surviving samples.

Figure 1 shows the surviving samples on the signal

**Table 1.** Parameter regions for  $2\sigma$  ( $\chi_{\gamma\gamma+\tau\tau+bb}^2 \leq 8.03$ ) and all surviving samples.

	$2\sigma$ samples	all surviving samples
$\lambda$	0.11–0.58	0.10–0.69
$\kappa$	–0.60–0.55	–0.56–0.61
$\tan\beta$	6.4–45.2	2.6–50.6
$\mu_{\text{eff}}/\text{GeV}$	139–487	102–978
$M_0/\text{TeV}$	0–9.5	0–10.0
$A_0/\text{TeV}$	–5.0–6.5	–8.3–9.3
$M_1/\text{GeV}$	–805–199	–1000–993
$M_2/\text{TeV}$	–6.7–1.0	–10.0–2.4
$M_3/\text{TeV}$	–3.4–6.4	–4.8–9.8
$A_\lambda/\text{TeV}$	1.4–10.0	0.1–10.0
$A_\kappa/\text{TeV}$	–2.0–2.4	–2.7–2.7

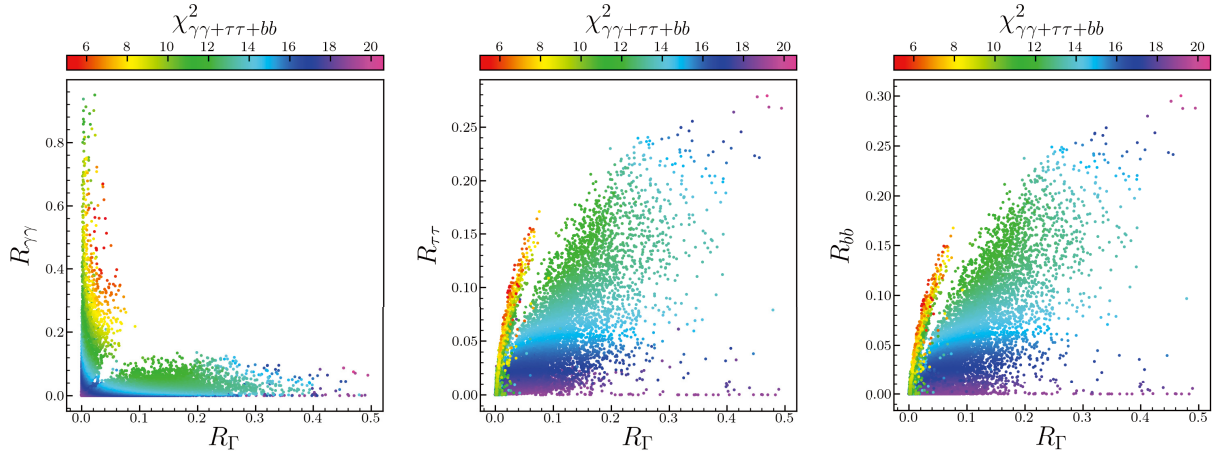
strengths  $R_{\gamma\gamma}(gg \rightarrow h_1 \rightarrow \gamma\gamma)$ ,  $R_{\tau\tau}(gg \rightarrow h_1 \rightarrow \tau\bar{\tau})$ , and  $R_{bb}(e^+e^- \rightarrow Zh_1 \rightarrow Zb\bar{b})$  versus width ratio  $R_\Gamma$  (total decay width of  $h_1$  divided by that of a SM Higgs of the same mass) planes, with colors denoting  $\chi_{\gamma\gamma+\tau\tau+bb}^2$ . This figure shows that the low-mass excess data are powerful in distinguishing the surviving samples. For the  $2\sigma$  samples,  $R_\Gamma \lesssim 0.1$ ,  $0.2 \lesssim R_{\gamma\gamma} \lesssim 0.8$ , and  $R_{\tau\tau}, R_{bb} \lesssim 0.2$ . The surviving samples can be clearly sorted into two regions:  $R_\Gamma \lesssim 0.1$  and  $R_{\gamma\gamma} \lesssim 0.2$ . Note that the  $2\sigma$  samples can be only located in the former. Hereafter, to compare with the  $2\sigma$  samples in the former region, we consider the  $3\sigma$  samples, or samples with  $8.03 \lesssim \chi_{\gamma\gamma+\tau\tau+bb}^2 \lesssim 14.16$  in the latter region, called small- $R_{\gamma\gamma}$  samples. Note from the middle and right planes that for the  $2\sigma$  samples,  $0.04 \lesssim R_{\tau\tau}, R_{bb} \lesssim 0.16$ , while for the small- $R_{\gamma\gamma}$  samples,  $0.05 \lesssim R_{\tau\tau}, R_{bb} \lesssim 0.25$ . In combination with experimental data, it can be observed that the  $2\sigma$  samples mainly fit well with the CMS di-photon excess, and small- $R_{\gamma\gamma}$  samples mainly fit well with the LEP  $Zb\bar{b}$  excess. The CMS di-tau excess has so large uncertainty that it cannot be dominant in our samples.

The signal strengths are related to the reduced couplings by

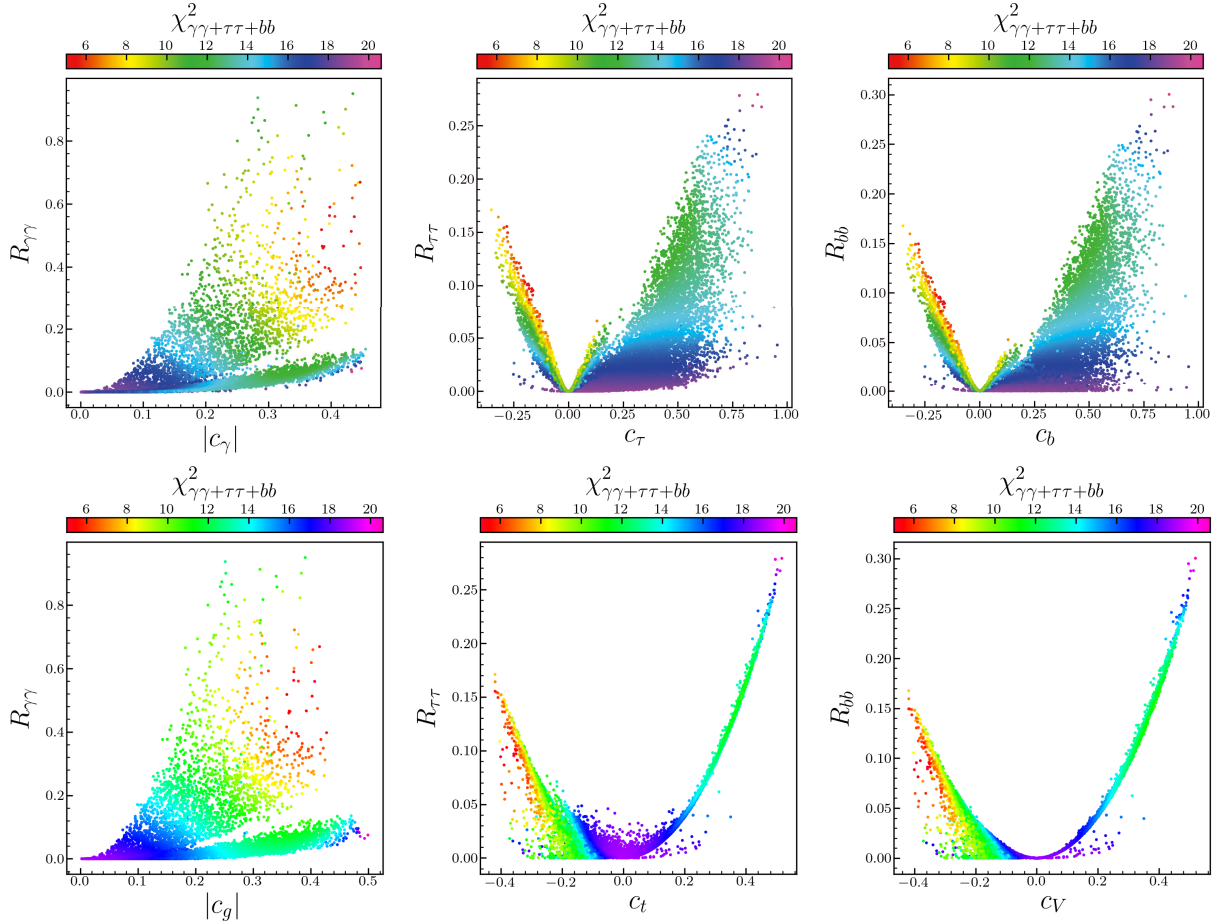
$$R_{\gamma\gamma} = c_g^2 c_\gamma^2 / R_\Gamma, \quad R_{\tau\tau} = c_g^2 c_\tau^2 / R_\Gamma, \quad R_{bb} = c_V^2 c_b^2 / R_\Gamma. \quad (11)$$

Figure 2 shows the surviving samples on the signal strengths versus reduced coupling planes, with colors denoting again  $\chi_{\gamma\gamma+\tau\tau+bb}^2$ . Note that the reduced couplings can be sorted into two classes:  $|c_\gamma| \approx |c_g| \approx |c_t| \approx |c_V|$  and  $c_b \approx c_\tau$ . Note also that the width ratio is determined by  $c_b^2$ , and the dominant branching ratio of the light scalar is that

<sup>1)</sup> We calculate Higgs masses and their mixing with the most complete calculation implemented in NMSSMTools, which includes full one-loop and dominant two-loop corrections.



**Fig. 1.** (color online) Surviving samples on the planes of signal strength  $R_{\gamma\gamma}$  ( $gg \rightarrow h_1 \rightarrow \gamma\gamma$ ) (left),  $R_{\tau\tau}$  ( $gg \rightarrow h_1 \rightarrow \tau\bar{\tau}$ ) (middle),  $R_{bb}$  ( $e^+e^- \rightarrow Zh_1 \rightarrow Zb\bar{b}$ ) (right) versus width ratio  $R_{\Gamma}$ , respectively; the colours indicate  $\chi^2_{\gamma\gamma+\tau\tau+bb}$ .



**Fig. 2.** (color online) Same as in Fig. 1, but on the planes of signal strength versus reduced coupling:  $R_{\gamma\gamma}$  versus  $c_{\gamma}$  (upper left),  $R_{\gamma\gamma}$  versus  $c_g$  (lower left),  $R_{\tau\tau}$  versus  $c_{\tau}$  (upper middle),  $R_{\tau\tau}$  versus  $c_t$  (lower middle),  $R_{bb}$  versus  $c_b$  (upper right),  $R_{bb}$  versus  $c_V$  (lower right).

of  $b\bar{b}$ . The signal strengths can be approximately rewritten as

$$R_{\gamma\gamma} \approx c_t^4 / c_b^2, \quad R_{\tau\tau} \approx c_t^2, \quad R_{bb} \approx c_t^2, \quad (12)$$

where the small width ratio  $R_{\Gamma}$ , or approximate  $c_b^2$ , can increase the di-photon rate but cannot increase the  $b\bar{b}$  and di-tau rates. Thus,  $\chi^2_{\gamma\gamma+\tau\tau+bb}$  can be approximately expressed as

$$\chi_{\gamma\gamma+\tau\tau+bb}^2 \approx \left[ 25 \left( \frac{c_t}{c_b} \right)^4 + 311.8 \right] c_t^4 - \left[ 30 \left( \frac{c_t}{c_b} \right)^2 + 81.6 \right] c_t^2 + 19.0. \quad (13)$$

According to Fig. 2, for  $2\sigma$  samples, the light scalar has negative reduced couplings to fermions and  $W/Z$  bosons, with  $0.3 \lesssim -c_t \lesssim 0.4$  and  $0.05 \lesssim -c_b \lesssim 0.3$ ; for small- $R_{\gamma\gamma}$  samples, the reduced couplings are positive, with  $0.25 \lesssim c_t \lesssim 0.45$  and  $0.25 \lesssim c_b \lesssim 1$ . Note also from Eq. (13) that when  $c_t = 0$  or  $c_t = 0.5$  with  $c_b = 1$ ,  $\chi_{\gamma\gamma+\tau\tau+bb}^2 \approx 19$ ; when  $|c_t| = 2|c_b| = \sqrt{0.1}$ ,  $\chi_{\gamma\gamma+\tau\tau+bb}^2 \approx 6$ .

Figure 3 shows the surviving samples on the  $S_{12}$ - $S_{11}$ ,  $\tan\beta$ - $S_{12}$  and  $c_t$ - $c_b$  planes. According to Fig. 3, when  $c_t, c_b \lesssim 0$ , or the couplings to quarks are flipped in sign,  $|c_t/c_b| \gtrsim 1$ , which defines the region where most  $2\sigma$  samples are located in; otherwise  $|c_t/c_b| \lesssim 1$ , and  $R_{\gamma\gamma}$  will be smaller. Combining Fig. 3 and Eq. (8), and given that

$\tan\beta \gg 1$  and  $|S_{12}| \ll 1$ , we can safely state that

$$c_V \approx c_t \approx S_{11}, \quad c_b \approx S_{12} \tan\beta. \quad (14)$$

It can also be observed from Fig. 3 that for the  $2\sigma$  samples,  $|S_{11}| \gg |S_{12}|$ , which means that the lightest Higgs boson is mainly mixed by the singlet and up-type doublet fields. Departing from this, in the wrong sign limit [72, 73] of the type-II two Higgs doublet model, the lighter Higgs boson is mixed by the up- and down-type doublets fields. We also checked that the absence of the case  $c_t \gtrsim c_b$  in Fig. 3 results from choosing a positive  $\mu_{\text{eff}}$ , which is favored by the muon  $g-2$  constraint. Given that the down-type doublet-like Higgs boson in NMSSM needs to be much heavier than the other two Higgs bosons to escape the constraints,  $S_{12}$ , or the mixing between singlet and down-type doublet, should be very small compared with  $S_{11}$ ; thus, the cases of  $c_t \lesssim 0$  and  $c_b \gtrsim 0$  are not

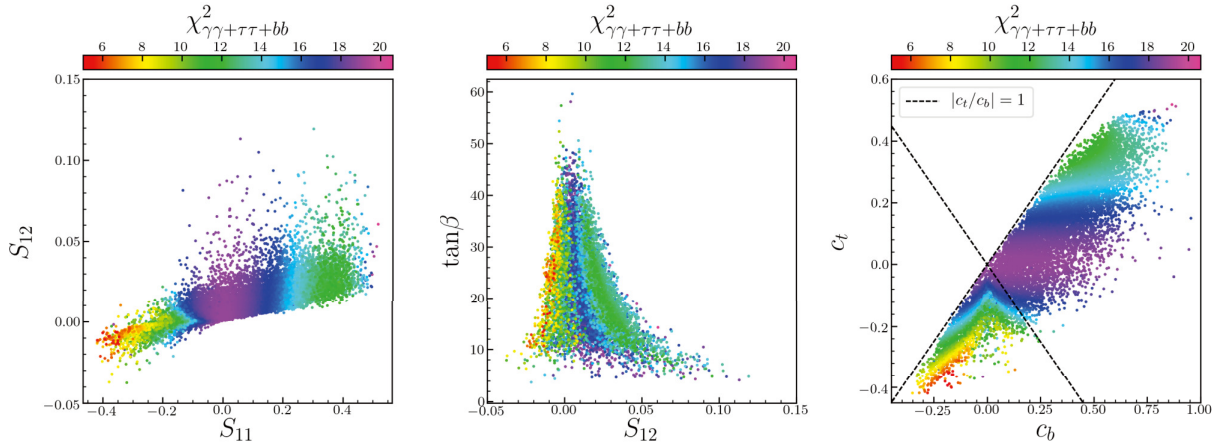


Fig. 3. (color online) Same as in Fig. 1, but on  $S_{12}$  versus  $S_{11}$  (left),  $\tan\beta$  versus  $S_{12}$  (middle), and  $c_t$  versus  $c_b$  (right) planes, respectively.

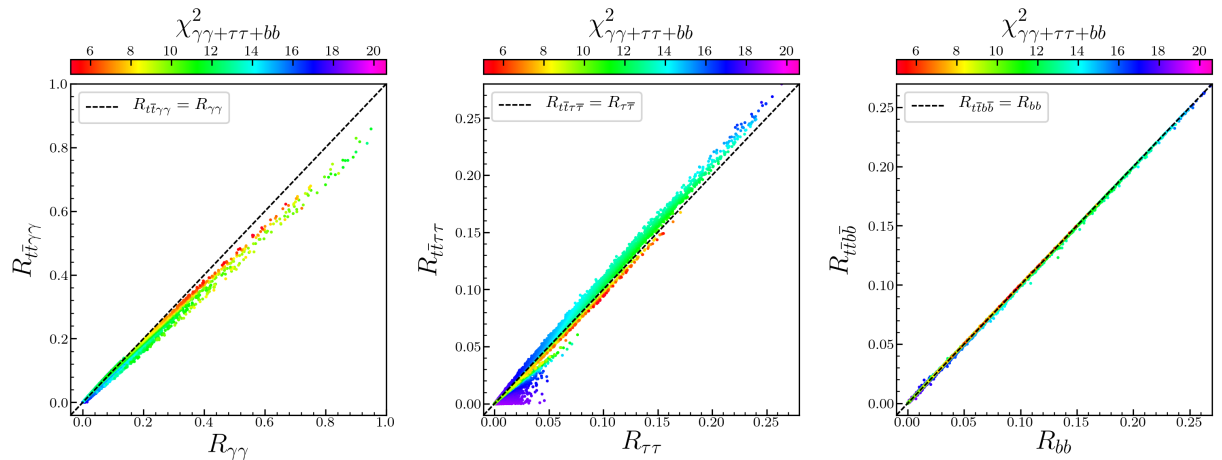


Fig. 4. (color online) Same as in Fig. 1, but on the planes of signal strengths in top-quark-pair associated channels versus those of existing excess channels:  $R_{t\bar{t}\gamma\gamma}$  versus  $R_{\gamma\gamma}$  (left),  $R_{t\bar{t}\tau\tau}$  versus  $R_{\tau\tau}$  (middle) and  $R_{t\bar{t}b\bar{b}}$  versus  $R_{b\bar{b}}$  (right) planes.



avored.

Considering that the mass region of excesses is close to the  $Z$  boson mass, we consider the scalar production associated with a top quark pair to reduce the backgrounds, with the signal strengths expressed as follows:

$$R_{i\bar{t}t\gamma\gamma} = c_t^2 c_\gamma^2 / R_\Gamma, \quad R_{i\bar{t}t\tau\tau} = c_t^2 c_\tau^2 / R_\Gamma, \quad R_{i\bar{t}tbb} = c_t^2 c_b^2 / R_\Gamma. \quad (15)$$

Figure 4 shows the surviving samples on the planes of signal strengths of top-quark-pair associated channels versus the three excess channels. Note that  $R_{i\bar{t}t\gamma\gamma} \approx R_{\gamma\gamma}$ ,  $R_{i\bar{t}t\tau\tau} \approx R_{\tau\tau}$ ,  $R_{i\bar{t}tbb} \approx R_{bb}$ . There is a small difference, especially between top-pair-associated and gluon-gluon-fusion channels. For  $2\sigma$  samples, the latter is slightly larger than the former; while for the small- $R_{\gamma\gamma}$  samples, the former is slightly larger than the latter. The difference comes from the contributions of squarks, and they are

**Table 2.** Eight benchmark points for the surviving samples.

	P1	P2	P3	P4	P5	P6	P7	P8
$\lambda$	0.315	0.348	0.335	0.271	0.297	0.165	0.116	0.339
$\kappa$	0.128	0.138	0.102	0.052	-0.121	-0.051	0.044	0.544
$\tan\beta$	30.8	30.5	31.8	25.1	21.2	6.4	11.1	14.7
$\mu_{\text{eff}}/\text{GeV}$	272	284	308	263	288	391	214	232
$M_0/\text{GeV}$	1503	1824	2342	1954	3415	303	790	335
$A_0/\text{GeV}$	1804	1947	867	1081	949	-1717	1653	1617
$M_1/\text{GeV}$	-49.6	-50.1	-19.7	-18.1	-83.9	-75.4	-63.7	-622
$M_2/\text{GeV}$	-2061	-2363	-3892	-2862	-302	249	-84	742
$M_3/\text{GeV}$	2877	3037	4948	4920	2992	1439	2004	2574
$A_\lambda/\text{GeV}$	7881	8510	8077	4474	6395	2212	2807	2745
$A_\kappa/\text{GeV}$	1610	2224	2111	837	1797	572	-107	-3538
$m_{h_1}/\text{GeV}$	96.5	95.0	95.2	95.6	98.3	96.9	98.8	96.4
$m_{h_2}/\text{GeV}$	124.9	125.2	126.0	125.7	125.9	125.7	126.1	126.0
$S_{11}$	-0.343	-0.340	-0.287	-0.255	-0.220	0.383	0.399	0.336
$S_{12}$	-0.0050	-0.0046	-0.0033	-0.0033	-0.0023	0.0695	0.0438	0.0405
$c_t$	-0.344	-0.341	-0.287	-0.256	-0.220	0.388	0.400	0.337
$c_V$	-0.343	-0.340	-0.287	-0.255	-0.220	0.390	0.401	0.338
$c_b$	-0.153	-0.139	-0.104	-0.082	-0.050	0.451	0.489	0.597
$c_\tau$	-0.153	-0.139	-0.104	-0.082	-0.050	0.451	0.489	0.597
$ c_g $	0.356	0.354	0.299	0.268	0.232	0.385	0.395	0.324
$ c_\gamma $	0.382	0.381	0.324	0.291	0.255	0.377	0.376	0.288
$R_\Gamma$	0.0200	0.0172	0.0107	0.0074	0.0046	0.1178	0.1396	0.1953
$R_{\gamma\gamma}$	0.548	0.618	0.510	0.472	0.455	0.106	0.096	0.026
$R_{\tau\tau}$	0.088	0.082	0.053	0.037	0.017	0.152	0.162	0.113
$R_{bb}$	0.083	0.077	0.049	0.035	0.016	0.156	0.167	0.123
$R_{i\bar{t}t\gamma\gamma}$	0.509	0.571	0.469	0.431	0.410	0.108	0.098	0.029
$R_{i\bar{t}t\tau\tau}$	0.082	0.076	0.049	0.034	0.016	0.155	0.166	0.123
$R_{i\bar{t}tbb}$	0.083	0.077	0.050	0.035	0.016	0.154	0.166	0.122
$\chi_{\gamma\gamma+\tau\tau+bb}^2$	5.37	5.50	6.87	7.91	9.26	10.95	11.42	12.96
$\chi_{125}^2$	116.4	116.7	103.8	99.1	95.7	99.2	99.4	90.9
$P_{125}$	0.344	0.337	0.673	0.784	0.850	0.782	0.777	0.919
$m_{\tilde{\chi}_1^0}$	44.53	46.01	43.15	43.00	60.38	43.92	44.98	227.96
$\Omega h^2$	0.0213	0.0719	0.0566	0.0187	0.0524	0.0862	0.0086	0.0065
$Br(h_2 \rightarrow \tilde{\chi}_1^0 \tilde{\chi}_1^0)$	0.0027%	0.0016%	0.022%	0.085%	0.15%	1.03%	0.028%	0.00%

positive or negative depending on  $c_t$ , that is, the reduced couplings to the top quark. The difference is small because of the high mass bounds of squarks [74] according to SUSY search results. As a comparison, new light colored particles can contribute significantly to the gluon-gluon-fusion channel [75].

Table 2 lists detailed information of eight representative benchmark points for further study, where  $\chi_{125}^2$  and  $P_{125}$  are the chi-square and  $P$  value from 125 GeV Higgs data of 111 groups (the number of degrees of freedom is 111). Note that for a SM Higgs of 125.09 GeV,  $\chi_{125}^2 = 89.7$  and  $P_{125} = 0.932$ . This table shows that it is difficult to satisfy the 125 GeV Higgs data and 95–100 GeV excesses simultaneously at the  $2\sigma$  level. For instance, concerning Point P4, for the 95–100 GeV excesses globally satisfied at the  $2\sigma$  level, the 125 GeV Higgs data can be at 78.4%, which is worse than that of a SM Higgs boson at 125 GeV.

Finally, we elaborate on dark matter, invisible Higgs decay, and electroweakino searches:

- For benchmark points P1-P7, the dark matter is bino-like, and the main annihilation mechanism is  $Z/h_2$  funnel. The mass of dark matter is different from  $M_1$  because the parameters  $M_{1,2,3}$  are defined at the GUT scale. There are correlations between parameters at GUT and SUSY scales, similar to those presented in Appendix A of a previous study of ours [55].

- We considered the constraint of invisible Higgs decay with the code HiggsBounds; the corresponding experimental data are provided in Refs. [76, 77]. For benchmark points P1-P7, the invisible Higgs decay  $Br(h_2 \rightarrow \tilde{\chi}_1^0 \tilde{\chi}_1^0)$  is approximately below 1%, because the large invisible ratios are not favored by both 125 and 95–100 GeV Higgs data.

- We also imposed constraints from SUSY searches with the code SModelS. For benchmark point P8, the dark matter is Higgsino-like and the main annihilation mechanism is  $W^\pm/Z$  exchanges. This point can escape the constraints from searches for electroweakinos in Ref. [78] because of its compressed mass spectrum and multiple decay modes. In the low mass region, it has SUSY particles such as Higgsino-like charginos and neutralinos of approximately 230 GeV, bino-like neutralino of 390 GeV, wino-like charginos and neutralinos of approximately 590 GeV,  $\tilde{\tau}_1$  of 246 GeV,  $\tilde{\nu}_\tau$  of 353 GeV,  $\tilde{\mu}_1$  of 478 GeV, and  $\tilde{\nu}_\mu$  of 472 GeV.

#### IV. CONCLUSIONS

In this study, we considered a light Higgs boson in the NMSSM to interpret the CMS di-photon and di-tau excesses, as well as the LEP  $b\bar{b}$  excess, in the

95–100 GeV mass region. We first scanned the parameter space and considered a series of constraints, including Higgs, dark matter, and SUSY searches. Then for each surviving sample, we calculated a chi-square considering its global fit to the three excess data. We focused on two respective types of samples:  $2\sigma$  and small- $R_{\gamma\gamma}$ . Finally, we drew the following conclusions:

- In NMSSM, it is difficult to satisfy the 95–100 GeV excesses simultaneously (not possible globally at  $1\sigma$  level, or simultaneously at  $2\sigma$  level).
- The global fit of the light Higgs boson to the three excesses is mainly determined by its couplings to up- and down-type fermions, which can be approximately expressed as in Eq. (13).
- The global  $2\sigma$  samples have negative reduced couplings to fermions and massive vector bosons, while they are positive for the small- $R_{\gamma\gamma}$  ones.
- The global  $2\sigma$  samples have a decay width smaller than one-tenth of the corresponding SM value, which can increase its di-photon rate but cannot increase its di-tau rate.
- The small- $R_{\gamma\gamma}$  samples can have  $Zb\bar{b}$  signal right fit to the LEP  $b\bar{b}$  excess, but have smaller di-photon and di-

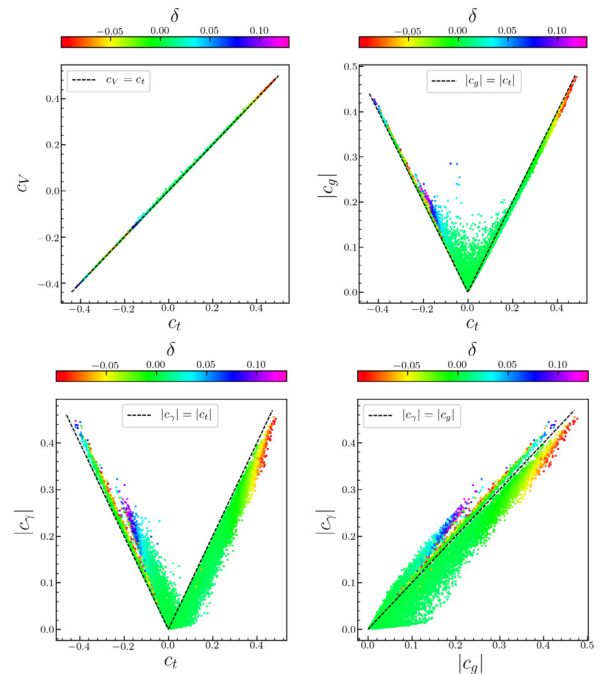


Fig. A1. (color online) Surviving samples on the planes of  $c_V$  (upper left),  $|c_g|$  (upper right) and  $|c_\gamma|$  (lower left) versus  $c_t$ , and  $|c_\gamma|$  versus  $|c_g|$  (lower right), with colors indicating the error ratio  $\delta$  between the approximated and complete ones in Eq. (13).

tau rates.

- The top-quark-pair associated signal strengths are nearly equal to those of the three exciting excesses, respectively.

### Appendix A: Error level of Eq. (13)

Fig. A1 shows the error level between the approximated chi-square and complete ones in Eq. (13). Note that  $c_V \approx c_t$  is a very good approximation. For most samples, given that the charged Higgs bosons and most SUSY

particles are heavy, their contributions to the loop-induced couplings  $c_g$  ( $c_\gamma$ ) are much smaller than those of the SM particles top quark (and  $W$  boson). Thus,  $c_g$  ( $c_\gamma$ ) are mainly determined by the coupling of the top quark,  $c_t$  (and that of the  $W$  boson,  $c_V$ ). Given that  $c_V \approx c_t$ , for most samples we have  $c_\gamma \approx c_V \approx c_t \approx c_g$ . According to Fig. A1, the error level between the approximate chi-square and complete ones in Eq. (13) are below 5% for most samples and approximately 15% at most for all. Therefore, Eqs. (12) and (13) are good approximations for most samples, with only two variable quantities.

### References

- [1] G. Aad *et al.* (ATLAS), *Phys. Lett. B* **716**, 1 (2012), arXiv:1207.7214[hep-ex]
- [2] S. Chatrchyan *et al.* (CMS), *Phys. Lett. B* **716**, 30 (2012), arXiv:1207.7235[hep-ex]
- [3] G. Aad *et al.* (ATLAS), *Nature* **607**, 52 (2022), arXiv:2207.00092[hep-ex]
- [4] S. Chatrchyan *et al.* (CMS), *Nature* **607**, 60 (2022), arXiv:2207.00043[hep-ex]
- [5] G. Aad *et al.* (ATLAS, CMS), *JHEP* **08**, 045 (2016), arXiv:1606.02266[hep-ex]
- [6] A. M. Sirunyan *et al.* (CMS), *Phys. Lett. B* **793**, 320 (2019), arXiv:1811.08459[hep-ex]
- [7] S. Chatrchyan *et al.* (CMS), (2022), arXiv:2208.02717[hep-ex]
- [8] R. Barate *et al.* (LEP Working Group for Higgs boson searches, ALEPH, DELPHI, L3, OPAL), *Phys. Lett. B* **565**, 61 (2003), arXiv:hep-ex/0306033
- [9] T. Biekötter, S. Heinemeyer, and G. Weiglein, *JHEP* **08**, 201 (2022), arXiv:2203.13180[hep-ph]
- [10] T. Biekötter, S. Heinemeyer, and G. Weiglein, (2022), arXiv:2204.05975[hep-ph]
- [11] S. Iguro, T. Kitahara, and Y. Omura, *Eur. Phys. J. C* **82**, 1053 (2022), arXiv:2205.03187[hep-ph]
- [12] S. Iguro, T. Kitahara, Y. Omura *et al.*, (2022), arXiv:2211.00011[hep-ph]
- [13] J. M. Cline, *Phys. Rev. D* **93**, 075017 (2016), arXiv:1512.02210[hep-ph]
- [14] J. Cao, X. Guo, Y. He *et al.*, *Phys. Rev. D* **95**, 116001 (2017), arXiv:1612.08522[hep-ph]
- [15] P. J. Fox and N. Weiner, *JHEP* **08**, 025 (2018), arXiv:1710.07649[hep-ph]
- [16] T. Biekötter, S. Heinemeyer, and C. Muñoz, *Eur. Phys. J. C* **78**, 504 (2018), arXiv:1712.07475[hep-ph]
- [17] U. Haisch and A. Malinauskas, *JHEP* **03**, 135 (2018), arXiv:1712.06599[hep-ph]
- [18] D. Liu, J. Liu, C. E. M *et al.*, *JHEP* **06**, 150 (2018), arXiv:1805.01476[hep-ph]
- [19] L. Liu, H. Qiao, K. Wang *et al.*, *Chin. Phys. C* **43**, 023104 (2019), arXiv:1812.00107[hep-ph]
- [20] W. G. Hollik, S. Liebler, G. Moortgat-Pick *et al.*, *Eur. Phys. J. C* **79**, 75 (2019), arXiv:1809.07371[hep-ph]
- [21] F. Domingo, S. Heinemeyer, S. Paßehr *et al.*, *Eur. Phys. J. C* **78**, 942 (2018), arXiv:1807.06322[hep-ph]
- [22] T. Biekötter, M. Chakraborti, and S. Heinemeyer, *Eur. Phys. J. C* **80**, 2 (2020), arXiv:1903.11661[hep-ph]
- [23] J. Cao, X. Jia, Y. Yue *et al.*, *Phys. Rev. D* **101**, 055008 (2020), arXiv:1908.07206[hep-ph]
- [24] J. M. Cline and T. Toma, *Phys. Rev. D* **100**, 035023 (2019), arXiv:1906.02175[hep-ph]
- [25] D. Sachdeva and S. Sadhukhan, *Phys. Rev. D* **101**, 055045 (2020), arXiv:1908.01668[hep-ph]
- [26] T. Biekötter, M. Chakraborti, and S. Heinemeyer, *Int. J. Mod. Phys. A* **36**, 2142018 (2021), arXiv:2003.05422[hep-ph]
- [27] J. A. Aguilar-Saavedra and F. R. Joaquim, *Eur. Phys. J. C* **80**, 403 (2020), arXiv:2002.07697[hep-ph]
- [28] T. Biekötter and M. O. Olea-Romacho, *JHEP* **10**, 215 (2021), arXiv:2108.10864[hep-ph]
- [29] S. Heinemeyer, C. Li, F. Lika *et al.*, *Phys. Rev. D* **106**, 075003 (2022), arXiv:2112.11958[hep-ph]
- [30] T. Biekötter, A. Grohsjean, S. Heinemeyer *et al.*, *Eur. Phys. J. C* **82**, 178 (2022), arXiv:2109.01128[hep-ph]
- [31] R. Benbrik, M. Boukidi, S. Moretti *et al.*, *Phys. Lett. B* **832**, 137245 (2022), arXiv:2204.07470[hep-ph]
- [32] R. Benbrik, M. Boukidi, and B. Manaut, (2022), arXiv:2204.11755 [hep-ph]
- [33] P. Fayet, *Phys. Lett. B* **64**, 159 (1976)
- [34] P. Fayet, *Phys. Lett. B* **69**, 489 (1977)
- [35] S. P. Martin, *Adv. Ser. Direct. High Energy Phys.* **18**, 1 (1998), arXiv:hep-ph/9709356
- [36] U. Ellwanger, C. Hugonie, and A. M. Teixeira, *Phys. Rept.* **496**, 1 (2010), arXiv:0910.1785[hep-ph]
- [37] M. Maniatis, *Int. J. Mod. Phys. A* **25**, 3505 (2010), arXiv:0906.0777[hep-ph]
- [38] J.-J. Cao, Z.-X. Heng, J. M. Yang *et al.*, *JHEP* **03**, 086 (2012), arXiv:1202.5821[hep-ph]
- [39] U. Ellwanger, *JHEP* **03**, 044 (2012), arXiv:1112.3548[hep-ph]
- [40] S. F. King, M. Mühlleitner, and R. Nevzorov, *Nucl. Phys. B* **860**, 207 (2012), arXiv:1201.2671[hep-ph]
- [41] Z. Kang, J. Li, and T. Li, *JHEP* **11**, 024 (2012), arXiv:1201.5305[hep-ph]
- [42] J. F. Gunion, Y. Jiang, and S. Kraml, *Phys. Lett. B* **710**, 454 (2012), arXiv:1201.0982[hep-ph]
- [43] R. Benbrik, M. Gomez Bock, S. Heinemeyer *et al.*, *Eur. Phys. J. C* **72**, 2171 (2012), arXiv:1207.1096[hep-ph]
- [44] S. F. King, M. Mühlleitner, R. Nevzorov *et al.*, *Nucl. Phys. B* **870**, 323 (2013), arXiv:1211.5074[hep-ph]
- [45] U. Ellwanger and C. Hugonie, *Adv. High Energy Phys.* **2012**, 625389 (2012), arXiv:1203.5048[hep-ph]



- [46] J. Cao, Z. Heng, J. M. Yang *et al.*, *JHEP* **10**, 079 (2012), arXiv:1207.3698[hep-ph]
- [47] K. Wang and J. Zhu, *JHEP* **06**, 078 (2020), arXiv:2002.05554[hep-ph]
- [48] J. Cao, F. Ding, C. Han *et al.*, *JHEP* **11**, 018 (2013), arXiv:1309.4939[hep-ph]
- [49] J. Huang, T. Liu, L.-T. Wang *et al.*, *Phys. Rev. Lett.* **112**, 221803 (2014), arXiv:1309.6633[hep-ph]
- [50] D. Curtin *et al.*, *Phys. Rev. D* **90**, 075004 (2014), arXiv:1312.4992[hep-ph]
- [51] S. Ma, K. Wang, and J. Zhu, *Chin. Phys. C* **45**, 023113 (2021), arXiv:2006.03527[hep-ph]
- [52] U. Ellwanger, J. F. Gunion, and C. Hugonie, *JHEP* **02**, 066 (2005), arXiv:hep-ph/0406215
- [53] U. Ellwanger and C. Hugonie, *Comput. Phys. Commun.* **175**, 290 (2006), arXiv:hep-ph/0508022
- [54] U. Ellwanger and C. Hugonie, *Comput. Phys. Commun.* **177**, 399 (2007), arXiv:hep-ph/0612134
- [55] F. Wang, K. Wang, J. M. Yang *et al.*, *JHEP* **12**, 041 (2018), arXiv:1808.10851[hep-ph]
- [56] P. Bechtle, S. Heinemeyer, T. Klingl *et al.*, *Eur. Phys. J. C* **81**, 145 (2021), arXiv:2012.09197[hep-ph]
- [57] P. Bechtle, S. Heinemeyer, O. Stål *et al.*, *Eur. Phys. J. C* **74**, 2711 (2014), arXiv:1305.1933[hep-ph]
- [58] P. Bechtle, D. Dercks, S. Heinemeyer *et al.*, *Eur. Phys. J. C* **80**, 1211 (2020), arXiv:2006.06007[hep-ph]
- [59] P. Bechtle, O. Brein, S. Heinemeyer *et al.*, *Eur. Phys. J. C* **74**, 2693 (2014), arXiv:1311.0055[hep-ph]
- [60] P. Bechtle, O. Brein, S. Heinemeyer *et al.*, *Comput. Phys. Commun.* **181**, 138 (2010), arXiv:0811.4169[hep-ph]
- [61] M. Tanabashi *et al.* (Particle Data Group), *Phys. Rev. D* **98**, 030001 (2018)
- [62] G. Hinshaw *et al.* (WMAP), *Astrophys. J. Suppl.* **208**, 19 (2013), arXiv:1212.5226[astro-ph.CO]
- [63] P. A. R. Ade *et al.* (Planck), *Astron. Astrophys.* **571**, A16 (2014), arXiv:1303.5076[astro-ph.CO]
- [64] E. Aprile *et al.* (XENON), *Phys. Rev. Lett.* **121**, 111302 (2018), arXiv:1805.12562[astro-ph.CO]
- [65] S. Kraml, S. Kulkarni, U. Laa *et al.*, *Eur. Phys. J. C* **74**, 2868 (2014), arXiv:1312.4175[hep-ph]
- [66] F. Ambrogio *et al.*, *Comput. Phys. Commun.* **251**, 106848 (2020), arXiv:1811.10624[hep-ph]
- [67] C. K. Khosa, S. Kraml, A. Lessa *et al.*, *LHEP* **2020**, 158 (2020), arXiv:2005.00555[hep-ph]
- [68] G. Alguero, J. Heisig, C. K. Khosa *et al.*, *JHEP* **08**, 068 (2022), arXiv:2112.00769[hep-ph]
- [69] A. M. Sirunyan *et al.* (CMS), *JHEP* **03**, 166 (2018), arXiv:1709.05406[hep-ex]
- [70] A. M. Sirunyan *et al.* (CMS), *JHEP* **03**, 160 (2018), arXiv:1801.03957[hep-ex]
- [71] R. L. Workman *et al.* (Particle Data Group), *PTEP* **2022**, 083C01 (2022)
- [72] P. M. Ferreira, J. F. Gunion, H. E. Haber *et al.*, *Phys. Rev. D* **89**, 115003 (2014), arXiv:1403.4736[hep-ph]
- [73] P. M. Ferreira, R. Guedes, J. F. Gunion *et al.*, in 2nd Large Hadron Collider Physics Conference (2014), arXiv:1410.1926[hep-ph]
- [74] K. Wang and J. Zhu, *Chin. Phys. C* **47**, 013107 (2023), arXiv:2112.14576[hep-ph]
- [75] J. Cao, P. Wan, J. M. Yang *et al.*, *JHEP* **08**, 009 (2013), arXiv:1303.2426[hep-ph]
- [76] G. Aad *et al.* (ATLAS), *Phys. Rev. D* **101**, 012002 (2020), arXiv:1909.02845[hep-ex]
- [77] A. M. Sirunyan *et al.* (CMS), *Eur. Phys. J. C* **79**, 421 (2019), arXiv:1809.10733[hep-ex]
- [78] G. Aad *et al.* (ATLAS), *Phys. Rev. D* **104**, 112010 (2021), arXiv:2108.07586[hep-ex]